Supplement information for

Unveiling the First Two Years Dataset on Atmospheric Deposition of Heavy Metals in Southern Vietnam Megacity: Potential Driving Factors and Ecological Risk Assessment

Ly Sy Phu Nguyen[1,2*], Le Quoc Hau[1,2], Vo Truong Gia Han[1,2], Tran Hoang Minh[1,2], Vo Thi Tam Minh[1,2], Tran Anh Ngan[1,2], To Thị Hien[1,2]

[1] Faculty of Environment, University of Science, Ho Chi Minh City, Viet Nam.

[2] Vietnam National University, Ho Chi Minh City, Viet Nam.

Corresponding email: Ly Sy Phu Nguyen (nlsphu@hcmus.edu.vn)

Text 1

Prior to each sampling, all collection equipment was rigorously pre-cleaned with 5% HNO_3, thoroughly rinsed with Milli-Q water, and air-dried for 24 hours to eliminate potential contaminants. After collecting and measuring the rainwater volume, each sample was preserved with 1% (v/v) HNO_3 in a 50 mL Falcon tube and stored at 4 °C until subsequent analysis. Samples were filtered using 0.45 μm PTFE filter and prepared for chemical analysis. To ensure analytical accuracy and minimize contamination, procedural blanks consisting of Milli-Q water were included and treated identically to the rainwater samples. Additionally, to assess potential contamination from the sampling apparatus, field blank samples (rinse the sampling kit with 100 mL Milli-Q) were collected using the same procedures but without exposure to the atmosphere. HM concentrations in all blank samples were shown in Table S1, indicating negligible contamination during sampling and handling.

Although this study focuses on the water-soluble fraction of HMs, which may lead to a certain underestimation of total deposition, the measured values remain representative of the overall pollution levels at the sampling site (HCMC). Existing studies have shown that water-soluble forms account for a substantial proportion of HMs in rainwater (e.g, 95% for Ni, 93% for Pb, 87% for Cd, and 80% for Cr)[1], supporting the validity of this approach. While pH variations can influence the partitioning between soluble and insoluble forms, particularly underestimating less soluble HMs such as Cd and Pb under neutral conditions, the water-soluble fraction reflects the more bioavailable and ecologically active portion. Moreover, acidifying the sample immediately after collection will help stabilize the pH and create uniformity in pH values between samples (i.e, same solubility potential for HMs between collected samples), improve accuracy, and limit the impact of pH on the solubility of HMs. Therefore, despite certain limitations, these

measurements provide a meaningful indicator of HMs contamination and can be effectively used to assess atmospheric deposition patterns.

Concentration of 8 HMs (Zinc (Zn), Manganese (Mn), Copper (Cu), Cr, Ni, Pb, Vanadium (V), and As) was quantified using Inductively Coupled Mass Spectrometry (ICP-MS) following the US EPA method 200.7 and the US EPA method 200.8. To investigate the potential sources of HMs contamination in rainwater, additional elements (i.e. Selenium (Se), Antimony (Sb), Calcium (Ca), and Iron (Fe)) were quantified using ICP-MS. Calibration was performed with standard solutions (1000 ppm, Merck), yielding calibration curves with correlation coefficients (R^2) ranging from 0.95 to 1.00. The method detection limit (MDL) was determined as follows: Zn (0.5 µg L^{-1}), Mn (0.3 µg L^{-1}), Cr (0.1 µg L^{-1}), Cu (0.3 µg L^{-1}), Ni (0.3 µg L^{-1}), Pb (0.03 µg L^{-1}), V (0.01 µg L^{-1}), and As (0.01 µg L^{-1}). Analytical precision was verified through repeated measurements of both standards and rainwater samples, showing relative standard deviations consistently below 5%. In addition, recovery tests using spiked samples were performed with spiked sample concentrations ranging from 2 - 50 µg L^{-1} (depending on HMs) and yielded recoveries of 90-105%, indicating good accuracy of the analytical method. More details for cleaning procedures, rainwater sample analysis, and quality assurance/quality control (QA/QC) protocols are detailed in Vo et al.[2]

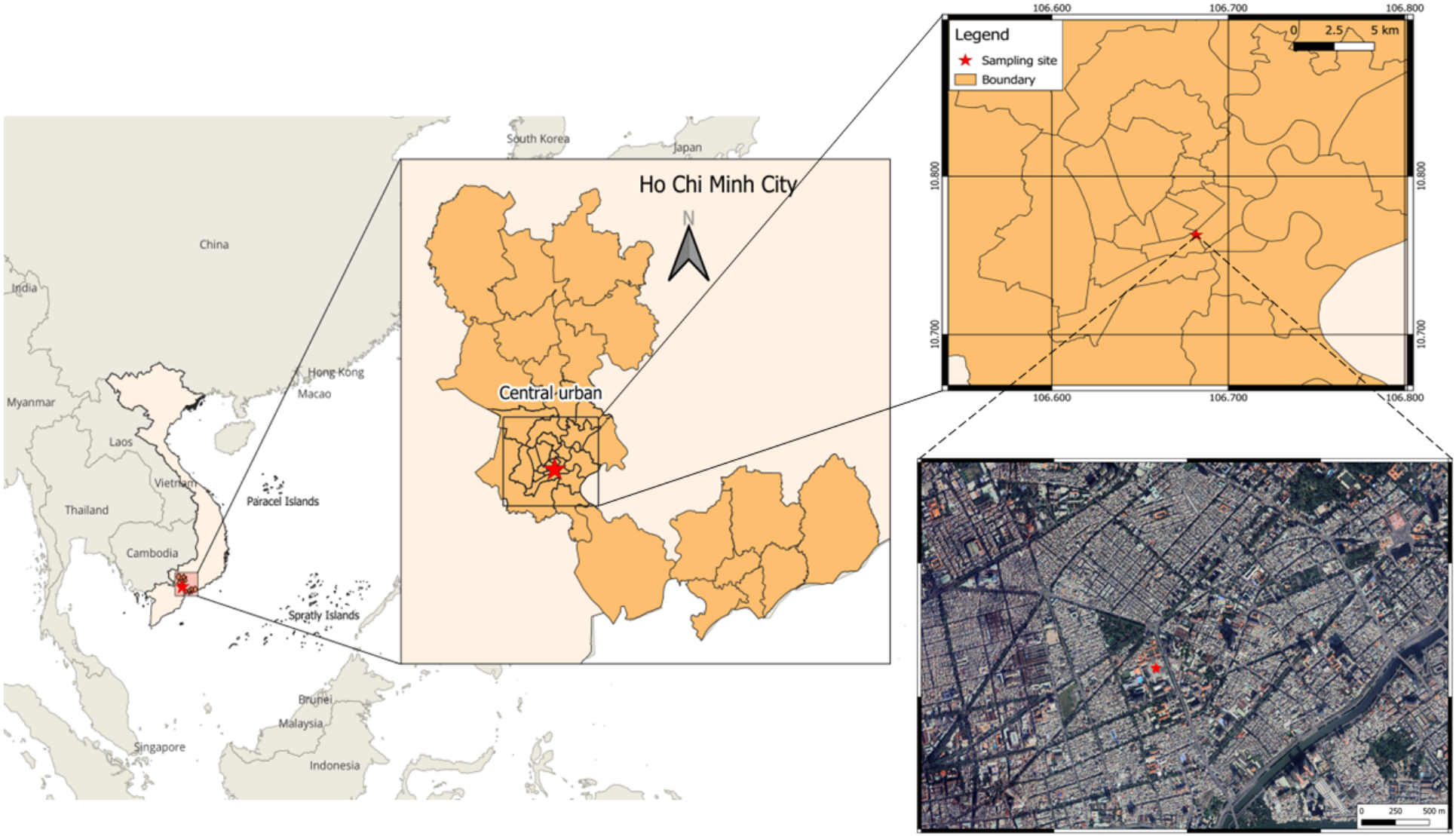

Fig. S1. Location of the sampling area (Ho Chi Minh City) and a Google map illustrates the urban area surrounding the sampling site.

Fig. S2. Bulk deposition samplers used for rainwater collection in Ho Chi Minh City (A) Schematic diagram and actual device; (B) The HDPE sampler.

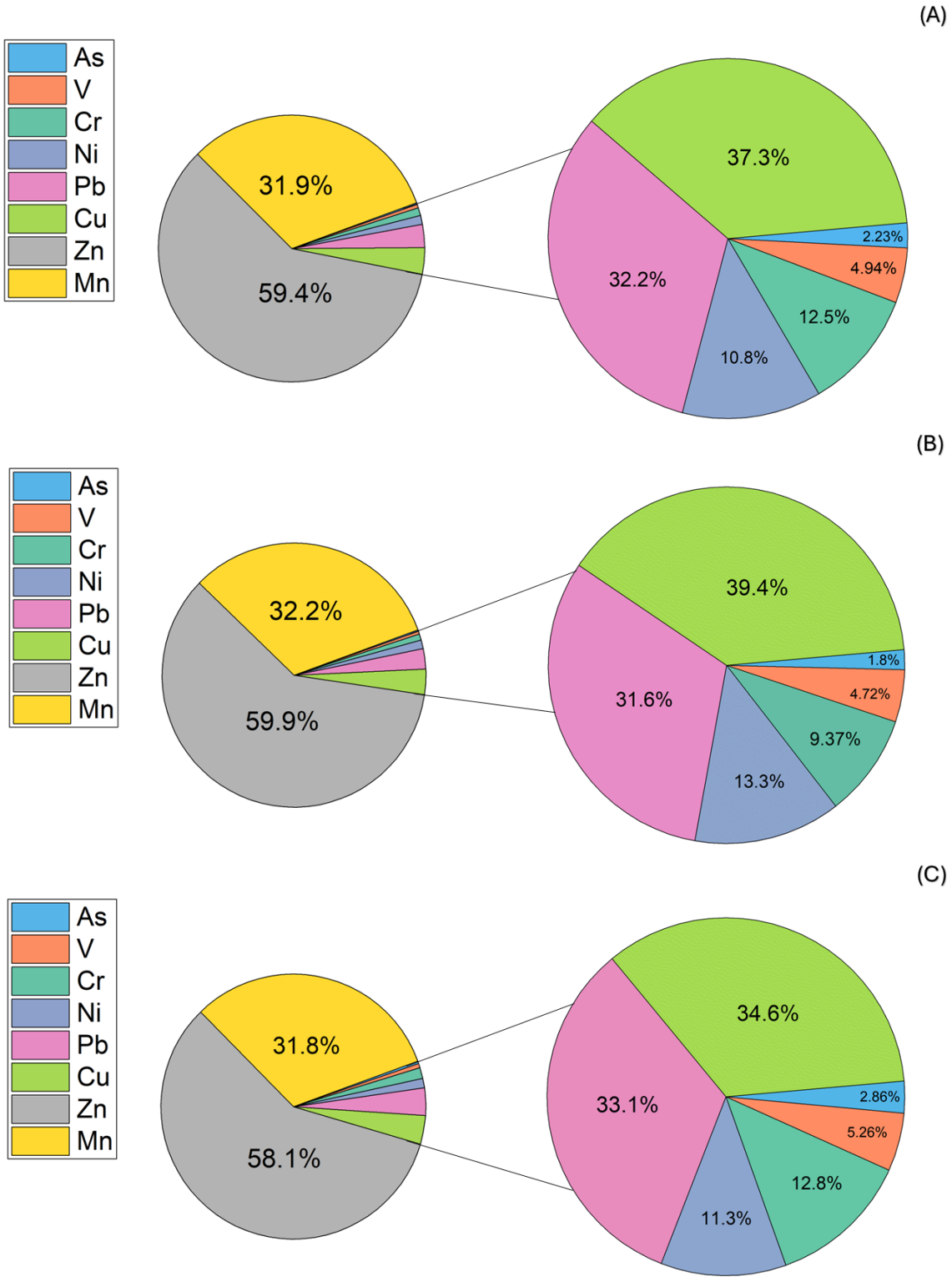

Fig. S3. Distribution of heavy metals (%) in (A) during the study period (2023-2024); (B) rainy season; and (C) dry season

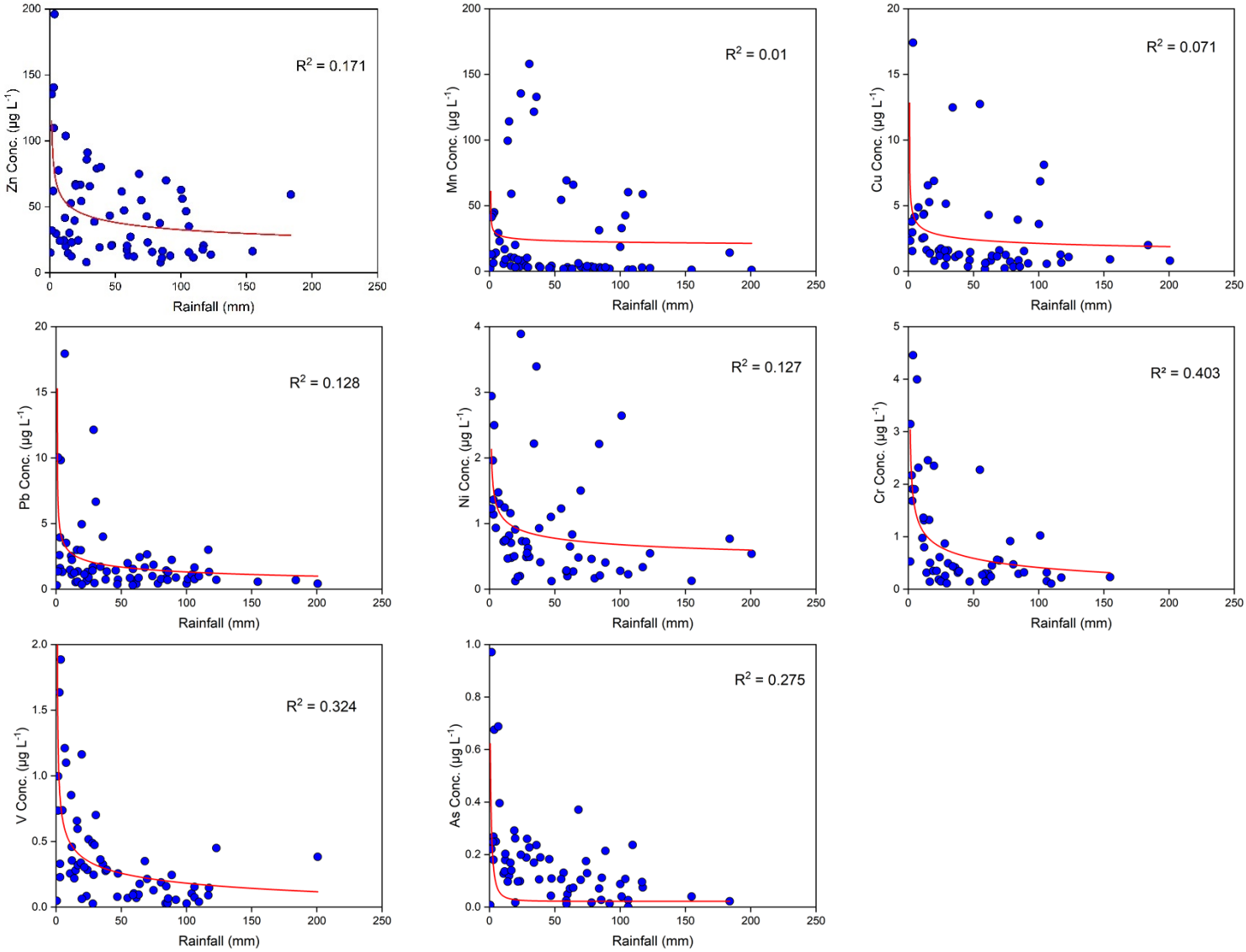

Fig. S4. Relationships between rainwater HMs concentration and rainfall amount

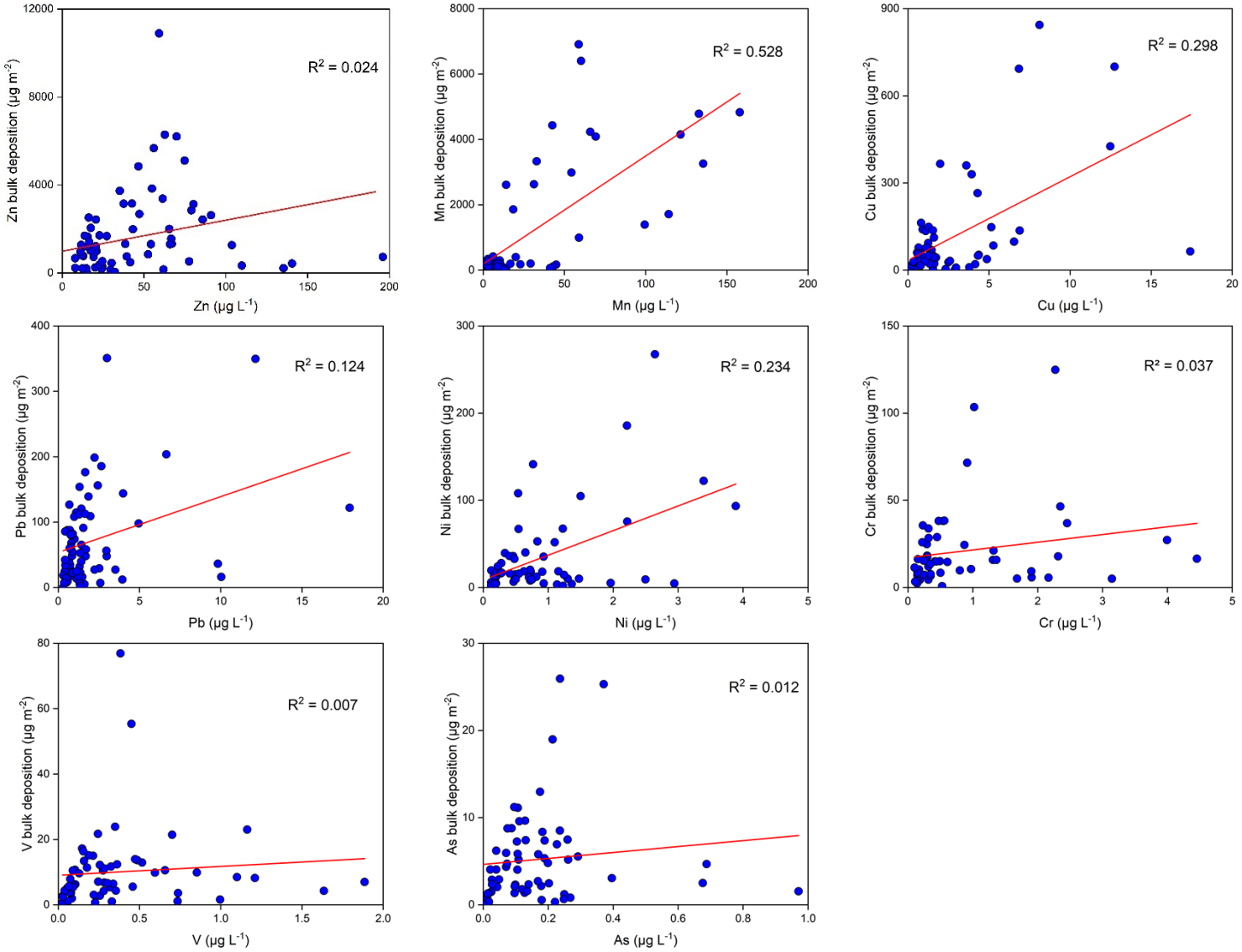

Fig. S5. Relationships between rainwater HMs concentration and bulk depositon flux

Table S1. Blank levels (mean ± S.D.) of selected HMs in this study

Heavy metal	Concentration (μg L^{-1})
Zn	3.63 ± 2.06
Mn	0.35 ± 0.25
Cu	0.34 ± 0.17
Pb	0.22 ± 0.12
Cr	0.12 ± 0.05
Ni	N.D.
V	N.D.
As	N.D.

Table S2. Classification criteria for ecological risk indices.

Parameters	Value range	Pollution degree
EF	EF < 1	No enrichment
	1 ≤ EF < 3	Minor enrichment
	3 ≤ EF < 5	Moderate enrichment
	5 ≤ EF < 10	Moderate severe enrichment
	10 ≤ EF < 25	Severe enrichment
	25 ≤ EF < 50	Very severe enrichment
	EF ≥ 50	Extremely severe enrichment
E_i	$E_r^i \leq 30$	Low risk
	$30 < E_r^i \leq 60$	Medium risk
	$60 < E_r^i \leq 120$	High risk
	$120 < E_r^i \leq 240$	Extremely high risk
	$E_r^i > 240$	Serious risk
RI	$RI \leq 60$	Low risk
	$60 < RI \leq 120$	Medium risk
	$120 < RI \leq 240$	High risk
	$RI > 240$	Extremely high risk

Note: E_r^i is the single factor potential ecological risk index, RI is comprehensive potential ecological risk index.

Table S3. Summary of rain depths, rainwater HM concentrations, and bulk deposition fluxes at HCMC during the study period.

Date	Sample size	Rain depth (mm)	Variable	Zn	Mn	Cu	Pb	Ni	Cr	V	As
2023	34	1739.8	VWM (μg L^{-1})	43.1	28.3	3.26	1.31	0.98	0.54	0.15	0.11
			Bulk deposition flux (μg m^{-2} $year^{-1}$)	75025.9	49255.9	5673.9	2272.1	1703.3	939.9	257.8	184.9
2024	36	1970	VWM (μg L^{-1})	22.7	15.8	1.05	1.73	0.43	0.30	0.22	0.08
			Bulk deposition flux (μg m^{-2} $year^{-1}$)	44745.0	31046.0	2070.5	3407.6	839.9	591.5	441.1	162.4
All	70	1854.9	VWM (μg L^{-1})	32.9	22.0	2.16	1.52	0.70	0.42	0.19	0.09
			Bulk deposition flux (μg m^{-2} $year^{-1}$)	59885.4	40150.9	3872.2	2839.8	1271.6	765.7	349.4	173.7

Table S4. Summary of HMs concentrations (μg L^{-1}) at HCMC and various sites worldwide.

Sites	Type	Period	Zn	Mn	Cu	Pb	Ni	Cr	V	As	Reference
HCMC, Vietnam	Urban	2023-2024	32.9	22.0	2.16	1.52	0.7	0.42	0.19	0.09	This study
Kolkatai, India	Urban	2019	31	14	4.1	1.0	3.7	0.82	0.76	-	3
Dinajpur, Bangladesh	Urban	2017	535.6	15.3	9.5	1.6	5.5	0.21	0.59	0.34	4
Sylhet, Bangladesh	Urban		177.1	6.2	7.1	2.8	15.3	0.12	0.23	0.31	
Singapore	Urban	2000	7.23	2.78	5.58	3.37	3.86	1.62	3.54	-	5
Zhanjiang Bay, China	Suburban	2021	13.02	-	1.16	29.3	-	-	-	0.18	6
Central Himalayas, China	Remote	2009-2010	0.47	0.59	0.06	0.04	0.15	0.06	0.02	0.04	7
Jomsom, Nepal	Remote	2020	26.54	29.7	3.66	2.37	2.97	2.66	1.83	0.54	8
Nam Co, China	Remote	2007-2008	6.09	0.56	0.54	0.14	0.22	0.27	0.03	-	9
Cox's Bazar, Bangladesh	Remote	2017	19.0	1.8	1.0	6.3	0.72	0.16	0.15	0.14	4
Satkhira, Bangladesh	Remote		99.7	14.2	2.3	6.5	3.4	0.13	0.29	0.46	
Northeast Tibet, China	Remote	2018	1.2	3.5	1.5	0.14	1.4	9.2	0.48	3.1	10
Southeast Tibet, China	Remote	2009-2010	10.2	0.58	0.42	0.04	0.14	0.06	0.43	-	11
Lhasa, China	Remote	2010-2012	14.21	7.70	1.71	1.59	0.58	0.43	0.31	0.64	12
Chuncheon, Korea	Remote	2012	9.9	3.23	1.73	1.51	0.52	-	0.14	0.4	13
Multiple sites, China	Various	2019-2021	-	-	-	5.91	1.67	0.68	-	5.33	14

Table S5. Summary of HMs deposition (μg m^{-2} yr^{-1}) at HCMC and various sites worldwide.

Sites	Type	Period	Zn	Mn	Cu	Pb	Ni	Cr	V	As	Reference
HCMC, Vietnam	Urban	2023-2024	59885.4	40150.9	3872.2	2839.8	1271.6	765.7	349.4	173.7	This study
Dinajpur, Bangladesh	Urban	2017	938335	26890.2	16562	2840	9643	367.8	1034	593.8	4
Sylhet, Bangladesh	Urban		1052512	36771.8	42371	16938	90673	696.6	1349	1820	
Beijing, China	Urban	2016-2020	6180	40	560	12	530	410	160	650	15
Multiple sites, China	Urban	2019-2021	-	-	-	2500	1700	500	-	4400	14
Singapore	Urban	2000	18720	7280	14560	8840	10140	4160	9100	-	5
Guangzhou, China	Urban	2014-2015	162130	-	22230	17000	-	9860	-	-	16
Dinghushan, China	Suburban		185780	-	23060	42840	-	5960	-	-	
Zhanjiang Bay, China	Suburban	2021	12510	-	1070	38900	-	-	-	14000	5
Central Himalayas, China	Remote	2009-2010	134	168	17.1	10.4	41.8	15.8	6.75	12.3	6
Jomsom, Nepal	Remote	2020	3503.9	3927	482.8	313.1	391.4	351	241.4	71.8	7
Yangtze River Delta	Remote	2019-2020	295	-	115.3	-	48.3	130.14	-	-	17
Cox's Bazar, Bangladesh	Remote	2017	75.26	7226.5	3756	25008	2835	636.4	587.8	548	4
Satkhira, Bangladesh	Remote		192441	27380.2	4452	12549	6491	256.65	560.3	893.3	
Multiple sites, China	Remote	2019-2021	-	-	-	2200	1100	300	-	4000	14
Nam Co, China	Remote	2007-2008	266	297	231	60	97	139	33	-	9
Southeast Tibet, China	Remote	2009-2010	9183	520	377	32.3	126	54	385	-	11
Lhasa, China	Remote	2010-2012	5211	2423	584	516	171	118	353	233	12
Multiple sites, China	Remote	2019-2021	-	-	-	8100	1300	400	-	4800	14

Table S6. The HMs concentration (μg L^{-1}) for each cluster.

Cluster	V	Cr	Mn	Ni	Cu	Zn	As	Pb	Total
1	0.54	1.32	32.4	1.12	4.37	50.1	0.24	2.93	93.0
2	0.50	1.34	25.3	1.07	1.97	44.6	0.24	3.28	78.2
3	0.23	0.67	17.9	0.75	1.81	35.8	0.11	1.32	58.6
4	0.32	0.65	23.3	0.98	2.89	34.7	0.14	2.20	65.2

Table S7. Information of EFs of HMs in this study.

	HMs	**V**	**Cr**	**Mn**	**Ni**	**Cu**	**Zn**	**As**	**Pb**
EF	Average ± Stdev	3.64 ± 8.05	19.3 ± 40.4	22.0 ± 43.9	44.6 ± 126.8	90.2 ± 149.5	307.1 ± 293.4	57.9 ± 71.3	73.7 ± 143.1
	Min - Max	0.14 - 52.5	0.56 - 227.1	0.65 - 240.2	1.08 - 945.9	2.16 - 746.2	0.91 - 1181.0	1.12 - 400.6	3.91 - 978.9

Table S8. Correlation matrix of HMs concentrations in rainfall. The Upper shows the results, the lower shows *p*-values.

	Rain	Ni	Cu	Cr	Mn	Sb	As	Fe	Zn	Pb	V	Se	Ca	Temp
Rain	1.00	-0.19	-0.17	-0.13	-0.18	-0.22	-0.37	-0.41	-0.31	-0.32	-0.39	-0.36	-0.33	-0.47
Ni	0.07	1.00	0.80	0.84	0.76	0.52	0.39	0.22	0.41	0.37	0.36	0.29	0.21	0.01
Cu	0.10	0.00	1.00	0.81	0.82	0.50	0.24	0.19	0.35	0.34	0.27	0.08	-0.02	-0.01
Cr	0.15	0.00	0.00	1.00	0.76	0.57	0.42	0.23	0.45	0.51	0.42	0.32	0.15	-0.02
Mn	0.08	0.00	0.00	0.00	1.00	0.41	0.18	0.23	0.24	0.27	0.19	0.11	0.04	-0.01
Sb	0.04	0.00	0.00	0.00	0.00	1.00	0.65	0.30	0.50	0.81	0.43	0.32	0.28	0.13
As	0.00	0.00	0.03	0.00	0.07	0.00	1.00	0.54	0.59	0.76	0.67	0.61	0.18	0.19
Fe	0.00	0.04	0.07	0.03	0.03	0.01	0.00	1.00	0.55	0.43	0.64	0.39	0.36	0.19
Zn	0.01	0.00	0.00	0.00	0.03	0.00	0.00	0.00	1.00	0.52	0.40	0.46	0.26	0.03
Pb	0.01	0.00	0.00	0.00	0.02	0.00	0.00	0.00	0.00	1.00	0.56	0.48	0.38	0.11
V	0.00	0.00	0.02	0.00	0.07	0.00	0.00	0.00	0.00	0.00	1.00	0.36	0.40	0.37
Se	0.00	0.01	0.27	0.01	0.20	0.01	0.00	0.00	0.00	0.00	0.00	1.00	0.06	0.06
Ca	0.00	0.05	0.45	0.12	0.39	0.01	0.00	0.00	0.00	0.00	0.00	0.00	1.00	0.13
Temp	0.00	0.47	0.45	0.45	0.48	0.17	0.07	0.07	0.42	0.19	0.00	0.32	0.15	1.00

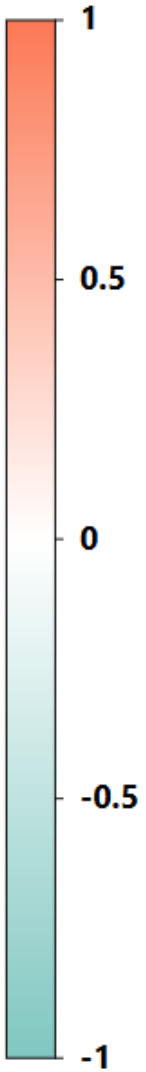

Table S9. The Total Variance Explained of PCA

Component	Total Variance Explained		
	Total	% of Variance	Cumulative %
1	5.138	39.525	39.525
2	2.024	15.566	55.091
3	1.291	9.932	65.022
4	1.082	8.327	73.349

Reference

1. Cizmecioglu, S.C., Muezzinoglu, A., 2008. Solubility of deposited airborne heavy metals. *Atmospheric Research* 89, 396–404. https://doi.org/10.1016/j.atmosres.2008.03.012
2. Vo, T.G.H., Nguyen, L.S.P., Trinh, P.D., Nguyen, C.M.D., Le, H.Q., 2024. Sampling and determination of metals in rainwater in Ho Chi Minh City. *Journal of Natural Sciences* 7, 80–93. https://doi.org/10.32508/stdjns.v7iS1.1360
3. Majumdar, A., Satpathy, J., Kayee, J., Das, R., 2020. Trace metal composition of rainwater and aerosol from Kolkata, a megacity in eastern India. *SN Applied Sciences* 2, 2122. https://doi.org/10.1007/s42452-020-03933-2
4. Adhikari, S., Zeng, C., Zhang, F., Adhikari, N.P., Gao, J., Ahmed, N., Khan, M.H.R., 2023. Atmospheric wet deposition of trace elements in Bangladesh: A new insight into spatiotemporal variability and source apportionment. *Environmental Research* 217, 114729. https://doi.org/10.1016/j.envres.2022.114729
5. Hu, G.P., Balasubramanian, R., 2003. Wet deposition of trace metals in Singapore. *Water, Air, and Soil Pollution* 144, 285–300. https://doi.org/10.1023/A:1022921418383
6. Hu, X., Xu, S., Deng, X., Wang, C., 2024. Temporal variation, sources, fluxes, and risk assessment of heavy metals and arsenic in rainwater from Zhanjiang Bay, Northern South China Sea: Impact of typhoons Lion and Kompasu. *Marine Pollution Bulletin* 209, 117077. https://doi.org/10.1016/j.marpolbul.2024.117077
7. Cong, Z., Kang, S., Zhang, Y., 2015. New insights into trace element wet deposition in the Himalayas: Amounts, seasonal patterns, and implications. *Environmental Science and Pollution Research* 22, 2735–2744. https://doi.org/10.1007/s11356-014-3496-1
8. Tripathee, L., Guo, J., Kang, S., Paudyal, R., Sharma, C.M., Huang, J., Sillanpää, M., 2020. Measurement of mercury, other trace elements and major ions in wet deposition at Jomsom: The semi-arid mountain valley of the Central Himalaya. *Atmospheric Research* 234, 104691. https://doi.org/10.1016/j.atmosres.2019.104691
9. Cong, Z., Kang, S., Zhang, Y., Li, X., 2010. Atmospheric wet deposition of trace elements to central Tibetan Plateau. *Applied Geochemistry* 25, 1415–1421. https://doi.org/10.1016/j.apgeochem.2010.06.011
10. Wei, T., Dong, Z., Kang, S., Zong, C., Rostami, M., Shao, Y., 2019. Atmospheric deposition and contamination of trace elements in snowpacks of mountain glaciers in the northeastern Tibetan Plateau. *Science of the Total Environment* 689, 754–764. https://doi.org/10.1016/j.scitotenv.2019.06.455
11. Liu, B., Kang, S., Sun, J., Zhang, Y., Xu, R., Wang, Y., Cong, Z., 2013. Wet precipitation chemistry at a high-altitude site (3,326 m asl) in the southeastern Tibetan Plateau. *Environmental Science and Pollution Research* 20, 5013–5027. https://doi.org/10.1007/s11356-012-1379-x
12. Guo, J., Kang, S., Huang, J., Zhang, Q., Tripathee, L., Sillanpää, M., 2015. Seasonal variations of trace elements in precipitation at the largest city in Tibet, Lhasa. *Atmospheric Research* 153, 87–97. https://doi.org/10.1016/j.atmosres.2014.07.030

13. Kim, J.E., Han, Y.J., Kim, P.R., Holsen, T.M., 2012. Factors influencing atmospheric wet deposition of trace elements in rural Korea. *Atmospheric Research* 116, 185–194. https://doi.org/10.1016/j.atmosres.2012.04.013
14. Ma, X., Sha, Z., Li, Y., Si, R., Tang, A., Fangmeier, A., Liu, X., 2024. Temporal-spatial characteristics and sources of heavy metals in bulk deposition across China. *Science of the Total Environment* 926, 171903. https://doi.org/10.1016/j.scitotenv.2024.171903
15. Pan, Y., Liu, J., Zhang, L., Cao, J., Hu, J., Tian, S., Xu, W., 2021. Bulk deposition and source apportionment of atmospheric heavy metals and metalloids in agricultural areas of rural Beijing during 2016–2020. *Atmosphere* 12, 283. https://doi.org/10.3390/atmos12020283
16. Ye, L., Huang, M., Zhong, B., Wang, X., Tu, Q., Sun, H., Chang, M., 2018. Wet and dry deposition fluxes of heavy metals in Pearl River Delta Region (China): Characteristics, ecological risk assessment, and source apportionment. *Journal of Environmental Sciences* 70, 106–123. https://doi.org/10.1016/j.jes.2017.11.019
17. Liu, P., Wu, Q., Hu, W., Tian, K., Huang, B., Zhao, Y., 2023. Effects of atmospheric deposition on heavy metals accumulation in agricultural soils: Evidence from field monitoring and Pb isotope analysis. *Environmental Pollution* 330, 121740. https://doi.org/10.1016/j.envpol.2023.121740